Supplement of Atmos. Chem. Phys., 22, 10061–10076, 2022
https://doi.org/10.5194/acp-22-10061-2022-supplement

Supplement of

Sulfuric acid in the Amazon basin: measurements and evaluation of existing sulfuric acid proxies

Deanna C. Myers et al.

Correspondence to: James N. Smith (jimsmith@uci.edu)

S1 Particle size distributions

Particle number size distributions measured during the observation period are shown in Figure S1 for particles with electrical mobility diameters 10 - 496 nm (5 - 16 February) and 11 - 460 nm (rest of campaign). Estimations of condensation sink were made from these measurements for the particle sizes measured during the entire campaign - (11 - 460 nm) using the method described in Kulmala et al. (2001) and (2012). Consistent with previous observations of increased accumulation mode particles (0.1 - 2.5 μm) during the dry season (IOP 2), higher concentrations in this size range are evident in Figure S1b.

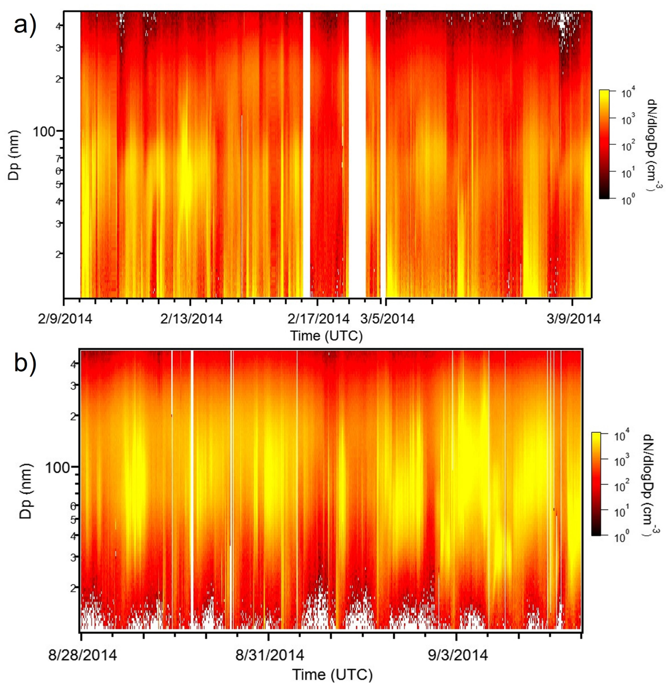

Figure S1. Particle number size distributions measured during IOP 1 (a) and IOP 2 (b). Note the time jump (2/19 to 3/5) on the IOP 1 time axis. Areas with white boxes represent periods where the instrument was not functioning properly.

S2 Comparison of Radiation with H_2SO_4, OH

To determine the pseudo rate constant k' for Proxy 2, we determined the linear fit between measured H_2SO_4 and the product of SO_2, global radiation, and CS^{-1} for the entire observation period (Fig. S2). The value of k' was found to be 2.43 x 10^{-10} m^2 s^1 W^{-1}. A poor correlation (R^2 = 0.59) was observed between the measured and estimated values, largely from the IOP 2 data.

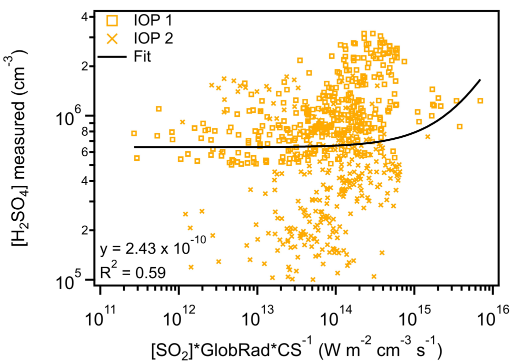

Figure S2. Measurements of H_2SO_4 for the entire observation period plotted against the product of SO_2, global radiation, and CS^{-1} to determine the pseudo rate constant k' for use in Proxy 2 (Fig. 2b). The line represents the linear fit to determine k'.

During both IOPs, but particularly IOP 2, there are many measurements of H_2SO_4 and OH when there is no radiation (GlobRad = 0) (Fig. S3), which can explain the poor correlation seen in Figure S2. These illustrate why Proxy 2 (Fig. 2b) does such a poor job estimating H_2SO_4, and why substituting radiation for OH can lead to order of magnitude underestimations.

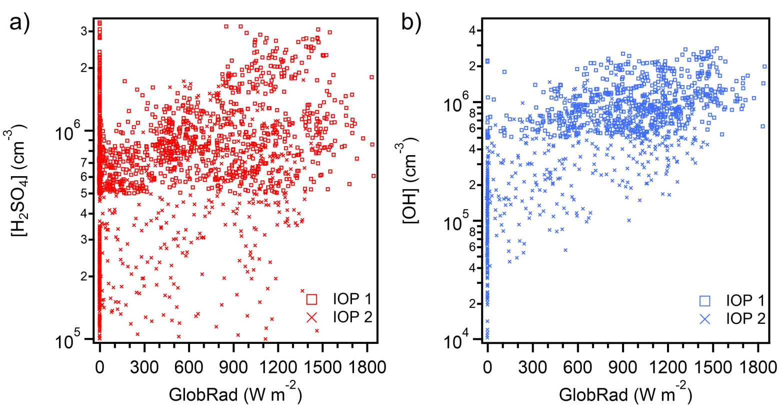

Figure S3. Comparison between measurements of (a) H_2SO_4 and (b) OH with global radiation. Note that there are numerous measurements of both species when global radiation was 0 W m^{-2}.

We also tested the best predictive proxy reported in Petäjä et al. (2009) (Fig. S4), which is very similar to Proxy 2 of this work. They only differ in the value of k' used in the estimation, which reflects the dependency of the proxy on radiation. While this proxy has improved estimations compared to Proxy 2, it still tends to underestimate measured H_2SO_4, particularly for IOP 2.

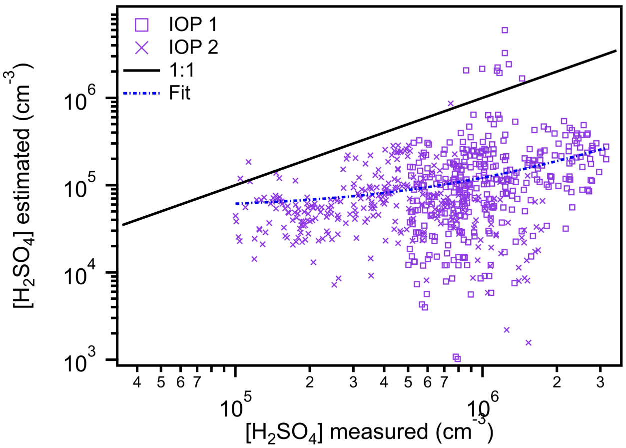

Figure S4. Estimated concentrations of sulfuric acid from the best predictive proxy reported in Petäjä et al. (2009) versus measured concentrations. Data from IOP 1 is plotted as boxes and data from IOP 2 is plotted as crosses. The 1:1 line is plotted to guide the eye. The fit line represents the fit between the measured and proxy-estimated values of sulfuric acid.

S3 Analysis of alkene concentration for Proxy 4

To determine if Proxy 4 would give a better nighttime estimate of H_2SO_4 if more alkenes were included in this proxy, we determined estimations using the combined concentrations of isoprene and monoterpene as the Alkene term. These results show there is minimal difference between the two estimations (Figs. S5 and S6), supporting the hypothesis that OH oxidation of SO_2 is also contributing to nighttime H_2SO_4 in this region.

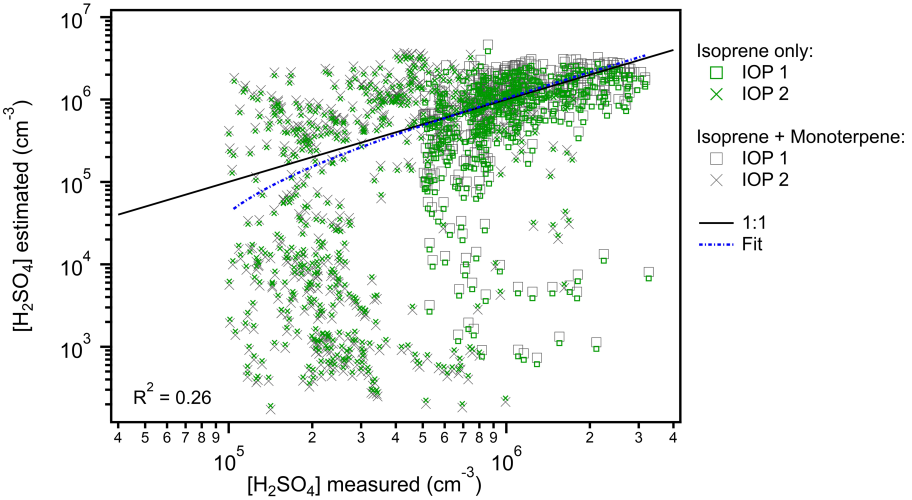

Figure S5. Estimations of sulfuric acid from Proxy 4 versus measured concentrations. Green points are estimates made only using the concentration of isoprene as the alkene term, and gray points used the combined concentration of isoprene and monoterpenes. Data from IOP 1 is plotted as boxes and data from IOP 2 is plotted as crosses. The 1:1 line is plotted to guide the eye. The fit line represents the fit between the measured and proxy-estimated values of sulfuric acid.

S4 Analysis of influence from Manaus on proxy estimates

To assess the differences in the proxy estimates between periods with influence from Manaus and those without, we used HYSPLIT back-trajectories to separate the data into those two categories (Rolph, et al., 2017; Stein, et al., 2015). The period including influence from Manaus accounted for $\sim$65 % of the measurements. We plotted the two-hour diurnal cycle of H_2SO_4, OH, O_3, and SO_2 to assess differences between the two periods (Fig. S7). The main differences in the trace gas concentrations between these two periods is that OH concentrations are about two times as large during times with influence from Manaus than those without, and O_3 concentrations are about 1.5 times larger. These are consistent with aircraft measurements made outside of Manaus, in which elevated levels of O_3 were found in plumes with emissions from Manaus (Kuhn, et al., 2010). Because the concentration of OH is higher at night during periods without Manaus influence, we hypothesize that Proxy 1 will provide better nighttime estimates during periods without this urban influence. This supports the model results from Lelieveld, et al. (2008), and Lelieveld, et al. (2016), which suggested secondary production of OH ton contribute substantially in the Amazon Basin. Additionally, the higher levels of O_3 and OH measured during the day in periods with influence from Manaus lead us to hypothesize that Proxies 1 and 4 will provide better daytime estimates during periods with influence form Manaus.

To test these hypotheses, we plotted the two-hour averaged diurnal variations of all the published proxies during periods with and without Manaus influence (Fig. S8). As expected, Proxy 1 does a better job estimating H_2SO_4 levels at night during periods without influence from Manaus (fig. S8b). Additionally, both Proxies 1 and 4 give better daytime estimates during times with influence from the city (Fig. S8a). Across both periods of influence, Proxies 3-5 provide the best daytime estimates.

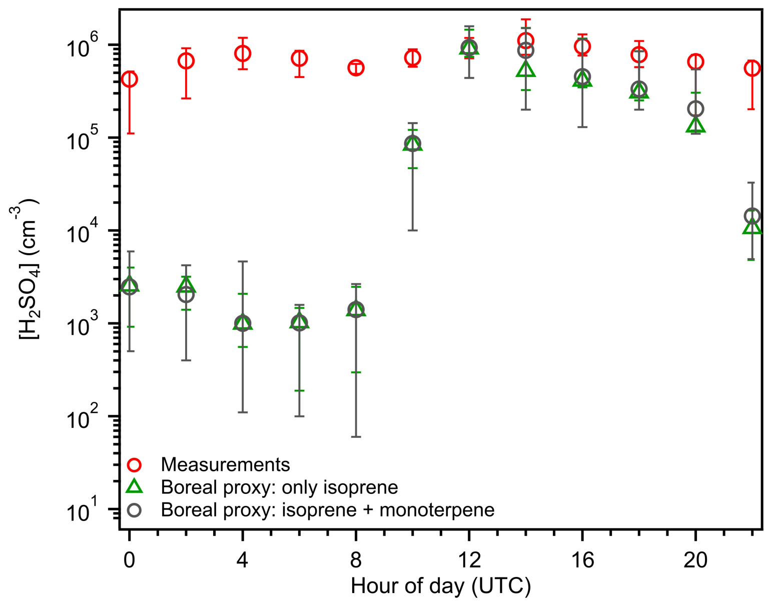

Figure S6. Two-hour averaged diurnal variation of the median sulfuric acid measurements (red), and estimations from Proxy 4 made using only isoprene concentrations (green), and using the combined isoprene and monoterpene concentrations (gray). Daylight hours: 08:00 - 22:00 UTC.

h

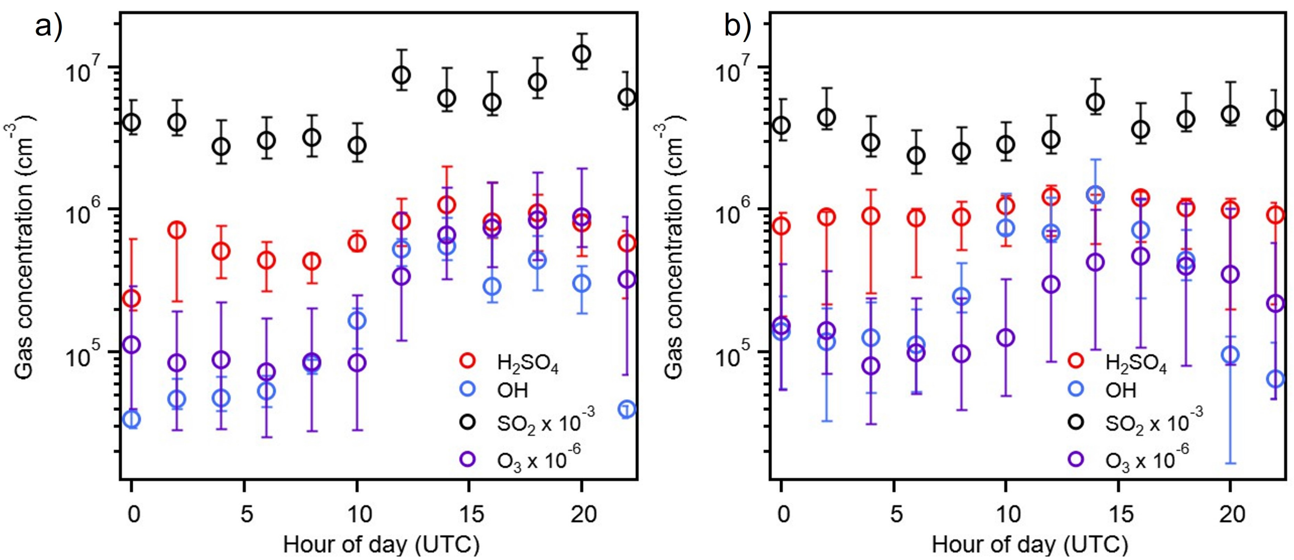

Figure S7. Two-hour averaged diurnal variation of the median H_2SO_4 (red), OH (blue), SO_2 (black), and O_3 (purple) during periods (a) with Manaus influence, and (b) without influence from Manaus. Daylight hours: 08:00 - 22:00 UTC.

At nighttime, Proxy 1 gives the best estimates when there is minimal influence from Manaus (Fig. S8b), though during periods with influence from Manaus both Proxies 1 and 4 give similarly accurate estimates.

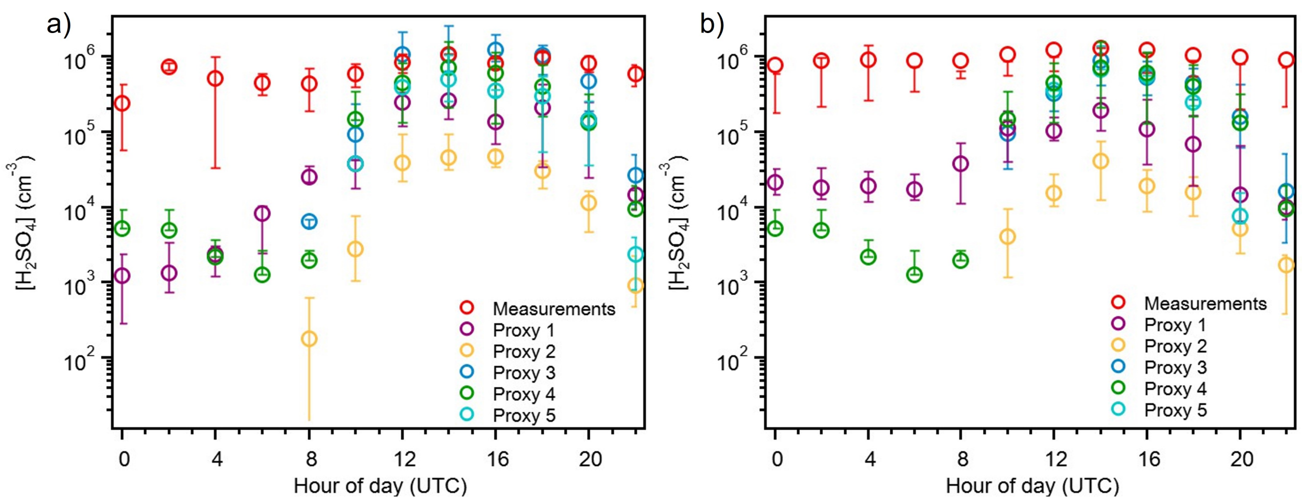

Figure S8. Two-hour averaged diurnal variation of the median H_2SO_4 measurements (red), and estimates made using Proxies 1 (purple), 2 (yellow), 3 (blue), 4 (green), and 5 (teal) during periods (a) with Manaus influence, and (b) without influence from Manaus . The bars represent the 25^{th} - 75^{th} percentiles for each value Daylight hours: 08:00 - 22:00 UTC.